Indian Journal of Pure & Applied Physics
Vol. 56, October 2018, pp. 802-813

Spectroscopic characterization and quantum chemical investigation of molecular structure and vibrational spectra of phthalazine-1(2H)-one

A Nataraj[a]*, T Beena[a], L Sudha[a], B Narayana[b] & V Balachandran[c]

[a]Department of Physics, S R M Institute of Science and Technology, Ramapuram, Chennai 600 089, India
[b]Department of Studies in Chemistry, Mangalore University, Mangalagnagotr 574 199, India
[c]Research Department of Physics, A A Government Arts College, Musiri, Tiruchirapalli 621 211, India

Received 4 July 2017; accepted 5 April 2018

In this study, vibrational and electronic transition analysis of phthalazine-1(2H)-one have been presented using experimental techniques FT-IR, FT-Raman and density functional theory (DFT) calculation. The structural properties of the molecule in the ground state have been calculated using DFT employing B3LYP/6-311++G(d,p) basis set. Optimized geometrical parameters have been interpreted and compared with the experimental values. The complete assignments have been performed on the basis of the experimental data and potential energy distribution (PED) of the vibrational modes. The calculated HOMO and LUMO energies and energy difference ($\Delta E_{\text{HOMO–LUMO}} = -4.876$ eV), confirm that charge transfers occur within the molecule. The stability of the molecule arising from hyperconjugative interactions and the charge delocalization has been analyzed using natural bond orbital's analysis (NBO). The specific heat, Gibb's free energy, and entropy of molecule have been calculated as a function of temperature by using statistical mechanics coupled with quantum chemical calculation. Observed vibrational wave numbers have been compared with calculated values, and found to be in agreement with experimental results. The study of dielectric properties like dielectric constant at microwave frequency, static dielectric constant and dielectric constant at optical frequency of Phthalazine-1(2H)-one have been determined. The dielectric relaxation studies provide information about the molecular structure and intermolecular interaction between phthalazine-1(2H)-one and alcohol mixture.

Keywords: Phthalazine-1(2H)-one, HOMO and LUMO, Hyperpolarizability, Molecular docking, Dielectric properties

1 Introduction

Phthalazine is a diazanaphthalene with two adjacent N atoms. Phthalazines are example of nitrogen hetero-cycles that possess exciting biological properties[1]. The numerous studies published on their applicability in different areas, especially as drugs[2]. Phthalazines have been reported to possess, anticonvulsant[3], cardio tonic[4], antimicrobial[5], antitumor[6-9], antihypertensive[10,11], antithrombotic, antidiabetic recently been reported to potentially inhibit serotonin reuptake and are considered anti-depression agents[13]. This compound has wide range of applications as therapeutic agents. Phthalazine and its derivatives possessing triazine nucleus have attracted great attention in recent years due to extensive variety of biological activity, particularly anticonvulsant activity. They are used as an intermediate in the synthesis of antimalarial drugs and its derivatives are used as antimicrobial agents. Thus, owing to the industrial and biological importance extensive spectroscopic studies on phthalazine were carried out by recording the FT-IR and FT-Raman spectra subjecting them to normal coordinate analysis. The dielectric relaxation studies of the molecule in polar solvent at different frequencies are expected to give a better understanding of the nature of molecular orientation processes[7,8].

Literature survey reveals that, to the best of our knowledge no complete vibrational analysis of calculations, and dielectric studies for phthalazine-1(2H)-one have been reported so far. In the present work, the experimental and theoretical FT-IR and FT-Raman spectra of phthalazine-1(2H)-one have been studied. The B3LYP level with 6-311++G (d,p) basis set have been performed to obtain the ground state optimized geometries and the vibrational wave numbers of the different normal modes as well as to predict the corresponding intensities for the different modes of the molecule and also to carry out HOMO-LUMO, polarizability, hyper polarizability, Mullikan's charge density and thermodynamical properties for the title

*Corresponding author (E-mail: sakuraj86@yahoo.co.in)

molecule. Finally, the dielectric properties of the compound help to provide valuable information for their applications in medicine and industrial research. Hydrogen bonds constitute a very interesting class of intermolecular interactions, which are of extreme importance in many fields of chemistry and molecular biology. The dielectric studies of phthalazine-1(2H)-one was carried out with the solvent ethanol in different concentration at 303 K.

2 Experimental Details

The crystalline sample of phthalazine-1(2H)-one was utilized for the FT-IR and FT-Raman spectral measurement. The FT-IR spectrum of title compound was recorded at room temperature in the region 4000–400 cm^{-1} at a resolution of ±1 cm^{-1} using BRUKER IFS 66V FT-IR spectrophotometer equipped with MCT detector, a KBr beam splitter and globar source were used. The FT-Raman spectrum was recorded on the same instrument with FRA 106 Raman accessories in the region 3500−100 cm^{-1}. The Nd:YAG laser operating at 200 mW power with 1064 nm, excitation was used as source. The static dielectric constant (ε_0) was measured by LCR meter supplied by M/s. Wissenschaijftlich Technische, Werkstatter, Germany. The measurement of dielectric constant at microwave frequency (ε') and dielectric loss (ε'') were carried out by X-Band microwave bench and the dielectric constant (ε_∞) at optical frequency was determined by Abbe's refractometer equipped by M/s.Vidyut Yantra, India.

3 Computational Methods

Quantum chemical calculations were carried out by means of the GAUSSIAN 03W program package[14] with Becke3-Lee-Yang-Parr (B3LYP)/DFT functional method with large 6-311++G(d,p) basis set[15]. The complete vibrational assignments are made with potential energy distribution (PED) calculation. The PED was done on a PC with the version V 7.0 – G77 of the MOLVIB program written by Tom Sundius[16,17].

4 Results and Discussion

4.1 Molecular geometry

The optimized molecular structure of phthalazine-1(2H)-one with numbering scheme of atoms obtained from Gaussview program[14] is shown in Fig. 1. The optimized structural parameters such as bond lengths, and bond angles of phthalazine-1(2H)-one molecule are determined by B3LYP level with 6-311++G(d,p) as basis set that were compared with closely

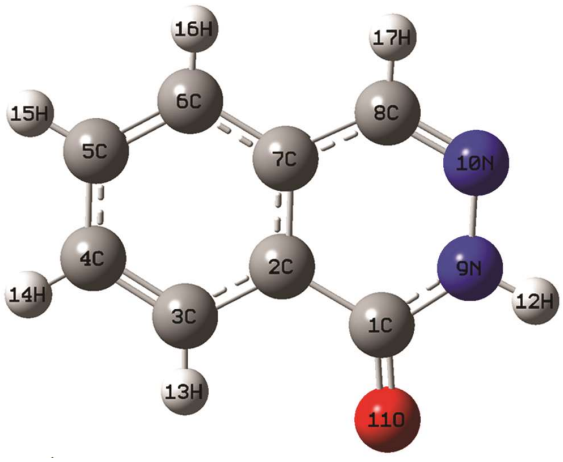

Fig. 1 — Optimized molecular structure of phthalazin-1(2H)-one.

experimental parameters obtained from the X-ray diffraction studies and also with phthalazine compound[18] shown in Table 1. The phthalazine-1(2H)-one is heterocyclic molecule and a resonance effect is observed in the ring of this molecule. As a result, C−C bond lengths and C−C−C bond angles in the two six members are similar as a dimer. In the benzene ring, C−C bond length is about 1.396 Å[18], our calculation were similar to this value, for example the optimized bond lengths of C−C in phenyl ring fall in the range 1.3844–1.4105 Å by B3LYP/6-311++G(d,p) level, show agreement with experimental data of 1.431 – 1.363 Å. The calculated value of N9−N10 (1.353 Å) is nearly correlated with experimental value (1.365 Å). The C−C range are slightly smaller than the calculated values of phthalazine, this because of intra-molecular interaction by the substitution of O atom in the title molecule. The density functional calculation gives almost same bond angles. From the theoretical results of our title molecule, we find that most of the optimized bond lengths and angles are slightly smaller as well as longer than the experimental value, this is due to the fact that the theoretical calculations belongs to isolated molecule in gaseous phase and experimental results belongs to molecule in solid state.

4.2 Molecular electrostatic potentials (MEP)

To predict reactive sites for electrophilic and nucleophilic attack for the investigated compound, molecular electrostatic potential (*MEP*) was calculated at B3LYP/6-311++G(d,p) optimized geometries. The strength of the electrostatic potential at the surface is represented by different colours; red represents

Table 1 — Optimized geometrical data of Phthalazine-1(2H)-one by DFT/B3LYP/6-311++G(d,p) method.

Parameters	Experimental bond lengths (Å)	Calculated bond lengths (Å)	Phthalazine* (DFT/B3LYP/ 6-11++G(d,p) bond lengths (Å)	Parameters	Experimental bond angles (°)	Calculated bond angles (°)	Phthalazine* (DFT/B3LYP/ 6-311++G(d,p) bond angles (°)
C1—O11	1.236	1.221		O11—C1—N9	121.06	113.3	
C1—N9	1.353	1.391	1.31	O11—C1—C2	123.59	125.9	
C1—C2	1.458	1.472		N9—C1—C2	115.34	113.3	115.9
C2—C3	1.392	1.4	1.31	C3—C2—C7	120.49	120.4	
C2—C7	1.395	1.41		C3—C2—C1	121.01	120.5	
C3—C4	1.370	1.385	1.423	C7—C2—C1	118.50	119.7	
C3—H13	0.973	1.083	1.087	C4—C3—C2	119.27	119.7	
C4—C5	1.388	1.404	1.414	C4—C3—H13	121.8	121.7	119.9
C4—H14	0.947	1.084		C2—C3—H13	118.9	118.6	
C5—C6	1.363	1.384	1.377	C3—C4—C5	120.64	120	124.4
C5—H15	0.96	1.084	1.084	C3—C4—H14	117.5	120	
C6—C7	1.404	1.407	1.415	C5—C4—H14	121.8	119	119.6
C6—H16	0.942	1.085	1.084	C6—C5—C4	120.76	120	119.6
C7—C8	1.431	1.442	1.377	C6—C5—H15	121.1	119.8	119.3
C8—N10	1.284	1.294	1.31	C4—C5—H15	118.1	119.7	119.6
C8—H17	0.975	1.085	1.085	C5—C6—C17	119.80	120	120.6
N9—N10	1.365	1.353	1.366	C5—C6—H16	122.7	120.5	120.8
N9—H12	0.92	1.011	1.088	C7—C6—H16	117.5	119.5	119.3
				C2—C7—C6	119.04	119.6	119.6
				C2—C7—C8	117.64	118.2	
				C6—C7—C8	123.32	122.6	120.6
				N10—C8—C7	124.93	123.8	124.6
				N10—C8—H17	115.4	115.7	115.4
				C7—C8—H17	119.7	120.5	120.8
				C1—N9—N10	127.55	128.7	119.5
				C8—N10—N9	116.01	116.9	119.5

*Bond length, and bond angles taken from Ref.[18]

region of the most electro negative potential, blue represents region of the most positive electrostatic potential and green represents region of zero potential. Potential decreases in the order red < orange < yellow < green < blue. The MEP surfaces provide necessary information about the reactive sites. The electron total density on to which the electrostatic potential surface has been mapped is shown in Fig. 2. The negative regions $V(r)$ were related to electrophilic reactivity, which are covered over the O10, N11 atoms and the positive one to nucleophilic reactivity, the region covered over the H atoms of phthalazine-1(2H)-one molecule. As easily can be seen in Fig. 2, this figure provides a visual representation of the chemically active sites and comparative reactivity of atoms[19].

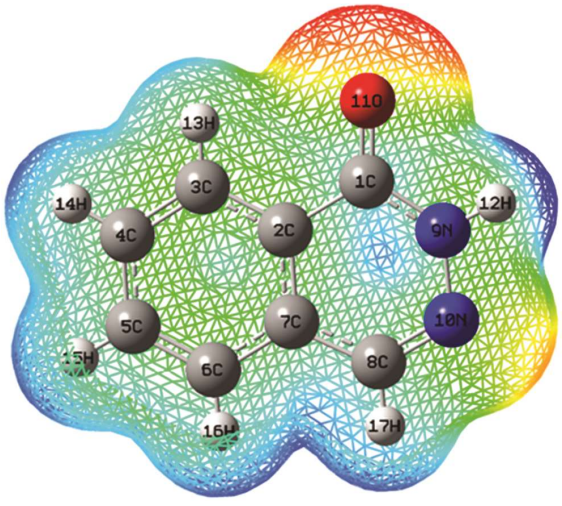

Fig. 2 — MEP map of phthalazine-1(2H)-one.

4.3 Frontier molecular orbital's (FMOs)

The HOMO, LUMO orbitals determine the way of molecule interacts with other species. The frontier molecular energy gap helps to characterize the chemical reactivity and kinetic stability of the molecule. A molecule with a small frontier orbital gap is more polarisable and is generally associated with a high chemical reactivity, low kinetic stability and is also termed as soft molecule[20].

The frontier molecular orbitals play an important role in the electric and optical properties[21]. The conjugated molecules are characterized by a small HOMO-LUMO separation, which is the result of a significant degree of intramolecular charge transfer from the end-capping electron acceptor groups through π–conjugated path[22]. The 3D plot of the frontier orbital's HOMO and LUMO of title molecule is shown in Fig. 3. The positive phase is red and negative phase is green (for interpretation of the reference to colour in the text, the reader is referred to the web version of the article). The analysis of wave function indicates that the electron absorption corresponds to the transition from the ground state to the first excited state and is mainly described by one. An electron excitation from the high occupied molecular orbital is to the lowest unoccupied molecular orbital (HOMO-LUMO).

Generally, the energy gap between the HOMO and LUMO ($\Delta E_{\text{HOMO-LUMO}}$ = − 4.876 eV) is lesser, it is easier for the electrons of the HOMO (E_{HOMO} = − 6.843 eV) to be excited to LUMO when the energy of LUMO (E_{LUMO} = − 2.054 eV) is low.

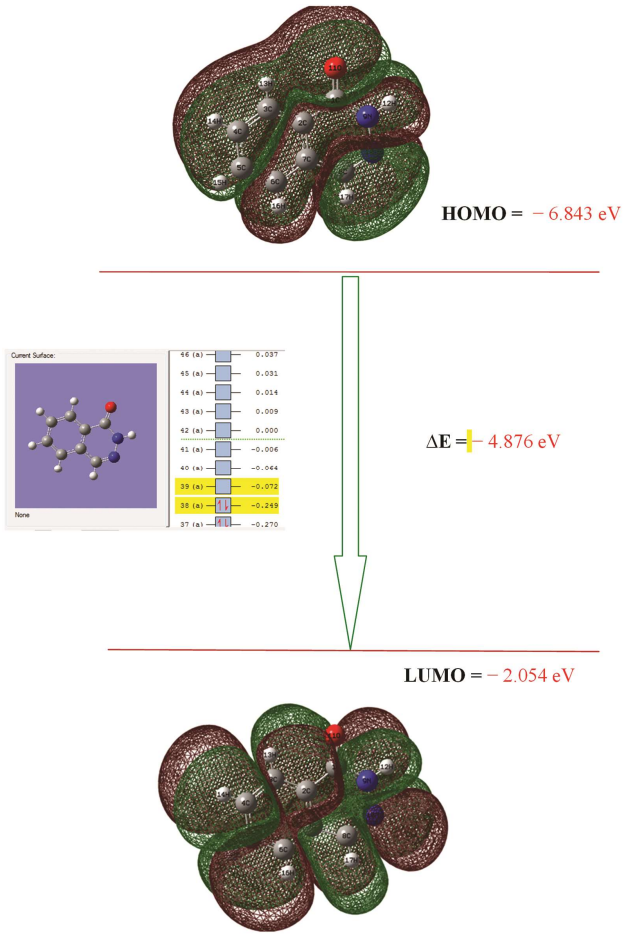

Fig. 3 — Calculated HOMO-LUMO structure of phthalazine-1(2H)-one.

The molecular electronegative (MEN) is good measure of the ability of attracting electrons to the molecule. The chemical hardness is a measure for resistance to deformation. It is very important tool to study the stability of molecular system. Pearson's maximum hardness principle (MHP) states that the minimum energy structure has the maximum hardness (η) and has been proved by the literature[23]. Parr *et al.* considered that the *EI* measures the second-order energy change of an electrophile as it is saturated with electrons[24].

It can be seen from the Table 2, that the ionization potential (*IP*) and electron affinity (*EA*) of title compound are − 6.843 eV and − 2.054 eV. The minimum electro negativity, electrophilicity index are – 4.445 eV, –2.0256 eV, respectively. The maximum chemical hardness and chemical potential values − 4.876 eV, and 4.445 eV, respectively. This may conclude that the title molecule has electronegative value and it is more reactive.

4.4 Natural bond orbital (NBO) analysis

NBO analysis has been performed on the phthalazine-1(2H)-one molecule at the B3LYP/ 6-311++G(d,p) level in order to elucidate, the intramolecular charge transfer (ICT) and delocalization of electron density within the molecule. The possibilities of electron density (ED) delocalization predicted between the lone pair donor atoms such as nN9, nN10, nO11, σN9–N10 to antibonding acceptor atoms such as π*C1–O11, π*C8–N10, π*C1–N9, π*C7–C8, π*C1–C2, π*C1–N9 of title molecule results intramolecular charge transfer which are possible and may cause stabilization of the system. The ICT may increase the electron density (ED) in lone pair of N9 and

Table 2 — Calculated physico-chemical properties for Phthalazine-1(2H)-one at B3LYP method.

Parameters	Values
HOMO energy ($-\varepsilon_{\text{HOMO}}$)	− 6.843 eV
LUMO energy ($-\varepsilon_{\text{LUMO}}$)	− 2.054 eV
HOMO-LUMO energy gap in eV	− 4.876 eV
Ionization potential (IP)	− 6.843 eV
Electron affinity (EA)	− 2.054 eV
Electrophilicity index (ω)	– 2.0256 eV
Chemical potential (μ)	4.445 eV
Electronegativity (χ)	– 4.445 eV,
Hardness (η)	− 4.876 eV

Table 3 — Second – order perturbation theory analysis of Fock matrix in NBO basis corresponding to the intra-molecular bonds of phthalazine-1(2H)-one molecule.

Donor (*i*)	ED (*i*) (*e*)	Acceptor (*j*)	ED (*j*) (*e*)	[a]$E^{(2)}$ (kJmol^{-1})	[b]$E_{(j)}$–$E_{(i)}$ (a.u.)	[c]$F_{(i,j)}$ (a.u.)
σC1–C2	1.975	σ*C6–C7	0.0236	3.12	1.23	0.55
σC1–N9	1.992	σ*C3–C3	0.0221	1.55	1.43	0.046
σC1–O11	1.991	σ*C1–C2	0.0617	2.54	1.49	0.056
σC2–C3	1.974	σ*C2–C7	0.0299	4.64	1.28	0.069
σC2–C7	1.97	σC2–C3	0.0221	4.13	1.28	0.065
σC3–H13	1.978	σC2–C7	0.0299	4.3	1.14	0.038
σC4–C5	1.979	σC5–C6	0.2715	3.04	1.31	0.056
σC6–C7	1.979	σC2–C7	0.0229	4.17	1.27	0.065
σC8–H17	1.974	σN9–N10	0.0277	6.41	0.94	0.069
σN9–H12	1.987	σC8–N10	0.0106	2.91	1.32	0.055
n N9	1.611	π*C1–O11	0.0108	61.71	0.29	0.121
		π*C8–N10	0.0106	31.18	0.28	0.088
n N10	1.938	π*C1–N9	0.0803	9.09	0.87	0.08
		π*C7–C8	0.0334	8.84	0.91	0.081
n O11	1.981	π*C1–C2	0.0617	16.32	0.71	0.098
		π*C1–N9	0.0803	24.45	0.71	0.119

O11atoms that weakens the respective bonds such as C1–N9 = 1.353 Å, C7–C8 = 1.431 Å, C1–C2 = 1.458 Å, the ED values are observed 0.0803 *e*, 0.0334 *e*, and 0.0617 *e*, respectively. Greater the value of $E(2)$, the more intensive is the interaction between electron donors and electron acceptors. Significant contributions for the molecular stabilization $E(2)$ are further given by the lone electron pair of nN9 to neighboring antibonding orbital of π*C1–O11 and π*C8–N10 leading to stabilization of 61.71 and 31.18 kJ mol^{-1}, respectively. The interaction energy related to the resonance in the molecule is electron withdrawing from the O11 atom (through π*C1–O11) to LP N9 leads to maximum stabilization energy of 61.71 kJ mol^{-1} is shown in Table 3. Hence the phthalazine-1(2H)-one structure is stabilized by these orbital interactions.

The charge distribution calculated by the Mulliken[25] and NBO method for the equilibrium geometry of title compound are visualized in Fig. 4. The charge distribution on the molecule has an important influence on the vibrational spectra. It is worthy to mention that NBO charges of C1, C2, C3, C4, C5, C6, C7, C8, N9, N10, O11 atoms exhibit negative charges and all hydrogen atoms exhibit positive charges. The above results show that the natural atomic charges are more sensitive to the changes in the molecular structure than Mulliken's net charges.

4.5 Molecular docking studies

The X-ray crystal structure of MET-477, GLU-475 was obtained from the protein data bank (PDB).

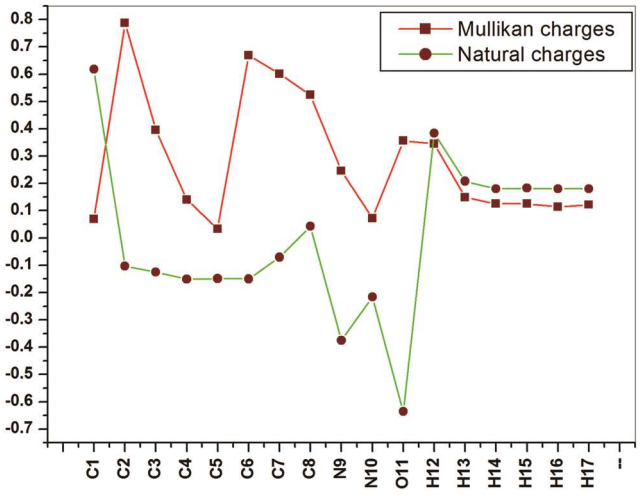

Fig. 4 — Comparative graph of calculated Mulliken's and Natural charges of phthalazine-1(2H)-one.

The compound docked well at the active sites of the target protein, when compared to the co-crystal ligand is confirmed by intermolecular bond lengths. The phthalazine-1(2H)-one molecule and co-crystal ligand shows comparable interactions with the residues. The residues MET-477, GLU-475 is interact with the phthalazine-1(2H)-one molecule at an average D…A distance of ~1.7 Å. Similarly, also in co-crystal ligand interact with same N-H residues at an average D…A distance of ~2.3 Å, these interactions visualized in Fig. 5.

4.6 Evaluation of dielectric parameters

According to Higasi[3], Average relaxation time τ(1) is described by:

$$\tau_{(1)} = \frac{a''}{\omega(a'-a_\infty)} \quad \ldots (1)$$

While the overall dielectric relaxation τ(2) is given by:

$$\tau_{(2)} = \frac{a_0 - a'}{\omega a''} \quad \ldots (2)$$

where "ω" the angular frequency a_0, a′, a″, a_∞ are defined by equation:

$$\varepsilon_0 = \varepsilon_{01} + a_0\omega_2 \quad \ldots (3)$$

$$\varepsilon' = \varepsilon_1' + a'\omega_2 \quad \ldots (4)$$

$$\varepsilon'' = a'' + \omega_2 \quad \ldots (5)$$

$$\varepsilon_\infty = \varepsilon_{1\infty} + a_\infty\omega_2 \quad \ldots (6)$$

in which subscript 1 refers to the pure solvent, 2 to the solute, subscript 0 refers to the static frequency and ∞ to the infinite or optical frequency and ω_2 is the weight fraction of the solute.

The experimental data of static dielectric constant (ε_0), microwave dielectric constant (ε′) optical dielectric constant (ε_∞) and relaxation time (τ) of the compound phthalazine-1(2H)-one in ethanol in various concentrations at 303 K are shown in Table 4. The static dielectric constant and optical dielectric constant increases with the increase in the concentration of phthalazine-1(2H)-one in the solvent ethanol. The increase in static dielectric constant in phthalazine-1(2H)-one suggests that a single volume effect arises from the solute particles which increase the ability of the molecule to orient in the applied field. The relaxation time increases with increasing solute concentration. The significant increase in the relaxation time (τ) values gives prominent information about the orientation of dipoles between the interacting components.

There are large numbers of alcohol molecules surrounding the phthalazine-1(2H)-one molecule, at high concentrations of alcohol in the mixtures. These associative alcohol molecules act as proton donors enabling hydrogen bonding with the solute molecules. Thus dipole-dipole interaction occurs between –OH group of alcohol with C=O of phthalazine-1(2H)-one. There is only small number of alcohol-molecule to enable the dipole-dipole interactions through hydrogen bonding with the non associative phthalazine-1(2H)-one molecule, at low concentration of alcohol mixtures. As a result weak intermolecular interaction occurs. The increase in concentration of the solute increases the relaxation time which directly depends upon the shape and size of the rotating molecular entities of the solution[26, 27].

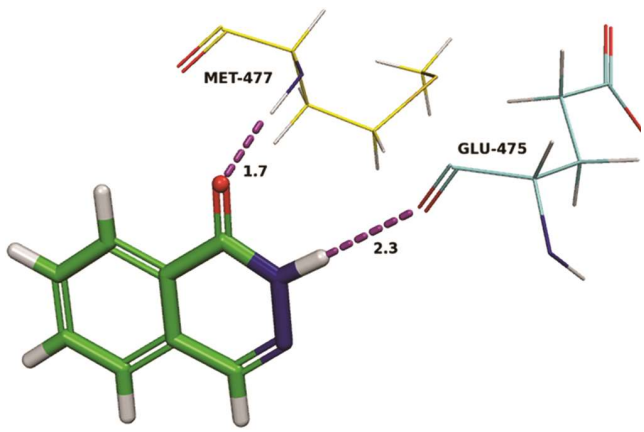

Fig. 5 — Molecular docking structure of phthalazine-1(2H)-one.

5 Vibrational Spectral Analysis

The optimized structure of phthalazin-1(2H)-one were used to compute the vibrational wave numbers at the DFT (B3LYP)/6-311++G(d,p) level of calculation. The molecule consists of 17 atoms, and belongs to C_1 point group symmetry. Hence the number of normal mode of vibrations for phthalazin-1(2H)-one works to 45. Of the 45 normal mode of vibrations are distributed as Γ_{vib} = 31 A' (in-plane) + 14 A"(out-of-plane).

All the 45 fundamental vibrations are active both in Raman scattering and in IR absorption. The calculated

Table 4 — Values of dielectric constant (ε0, ε′, ε∞) and relaxation time τ (ps) of phthalazine-1(2H)-one in ethanol at 303 K.

System	Concentration ethanol: Phthalazine-1(2H)-one	Static Dielectric constant (ε_0)	Microwave dielectric constant (ε′)	Optical dielectric constant (ε_∞)	Relaxation time (ps) (τ)
Ethanol + Phthalazine -1(2H)-one	1:3	2.8127	2.4685	2.2456	22.89
	1:2	2.9671	2.5668	2.2527	23.67
	1:1	3.1578	2.5943	2.2658	25.02
	2:1	3.2457	2.5618	2.2763	25.85
	3:1	3.3664	2.5246	2.2821	25.98

wave numbers are slightly higher than the observed values. The major factor which is responsible for these discrepancies is related to the fact that the experimental values are an anharmonic frequencies while the calculated values are harmonic frequencies. While anharmonicity is the main factor of the discrepancies in the case of vibrations related to the C–H and C–C in molecule, also in C=O bond, for other vibrations most of the discrepancies come from the approximate nature of the computational technique used and probably also from the lattice effects in the substance, studied as a solid.

The observed FT-IR and FT-Raman wave numbers for various modes of vibrations with PED assignments are also presented in Table 5. In discussing assignments, for the sake of brevity, only IR bands are used; where IR bands are not observed the Raman bands are used. Reference to computed bands are made in cases where there are no observed frequencies. Comparison of the wave numbers calculated at B3LYP level with the experimental values reveals the overestimation of the calculated vibrational modes due to neglect of anharmonicity in real system. Inclusion of certain extent makes the

Table 5 — Comparison of the experimental (FT–IR and FT–Raman) wavenumbers (cm^{-1}) and calculated wavenumbers (cm^{-1}) of phthalazine-1(2H)-one calculated by B3LYP method.

Mode numbers	Experimental		Calculated	Reduced mass (μ)	Force constant (*f*)	IR Intensity (I_{IR})	Raman activity	PED (%) ≥ 10 %
	FTIR	FT-Raman	Frequency					
1			121	6.105	0.053	1.869	2.989	γCCCC (68), γCCNN(25)
2		154 w	164	4.32	0.0693	0.2711	3.3135	γCCCO(45), γHCCH (35)
3			222	5.38	0.15	0.07	0.2706	γCCNN(57), γCCCC(26)
4		252 vw	285	6.439	0.308	0.438	0.330	γCCNN(45), γHCCH (35)
5		304 vw	420	3.249	0.338	2.751	0.393	γCCCC(48), βCCC (37)
6			468	4.8	0.61	0.03	0.653	γCCCC(67), γCCNN(26)
7		475 s	470	6.248	0.8148	0.6089	0.294	γCCCC(47), γHCCH (27)
8	490w	490 w	489	8.711	1.229	5.266	0.154	γCCCN (58), γCCCO(32)
9	562vs	545 w	551	7.03	1.26	9.99	0.0855	γHCCC (41), βCCC (38)
10	592vs	590 w	598	2.788	0.587	0.002	0.659	γCCCH (69), βCCO(25)
11	600s		599	8.321	1.757	2.473	0.723	γHCCH (55), βCHN (39)
12	681vs		667	1.9	0.4	14.45	1.2	γHCCH (57), βCCO(32)
13			717	1.990	0.604	121.96	7.96	γCCCH (55), βCHN (26)
14	720w	724 vs	727	6.416	1.999	2.801	1.917	γCHNO (45), γCCCH (35)
15	771vs		775	1.66	0.59	32.16	3.417	βCNN(47), βCCC (37)
16	797vs		803	2.853	1.085	4.945	0.883	βCCC (57)+ CC Ring breathing
17			804	6.155	2.347	22.349	0.525	βCCC (57), γCCCC(27)
18	862vw		887	1.28	0.59	7.97	5.551	βCCC (57), γCHNO (32)
19	879s		911	1.458	0.713	7.892	11.066	βCCC (61), γHCCH (35)
20	914s	913 w	924	4.826	2.431	23.583	0.470	βCCN (57), βCCC(36)
21	968ms		990	1.37	0.79	2.02	1.879	βCCO(58), γHCCC (25)
22	1019ms	1021 s	1017	1.317	0.803	0.1253	0.735	βCCH (69), νCCC (26)
23			1044	2.486	1.598	6.683	0.453	βCCH (69), νCCC (28)
24	1064ms		1096	3.45	2.44	12.43	15.942	νNN (62), βCCH(34)
25			1141	3.685	2.8276	32.229	5.784	βCCH (67), βCHN (25)
26	1152vs		1152	1.775	1.39	33.13	0.664	βCCH (64), βCHN (27)
27			1184	1.14	0.94	4.17	0.838	βCCH(57), νNN (31)
28	1233s	1233 vs	1248	2.005	1.842	12.571	6.063	βCCN (59), νOC(29)
29	1252s		1268	2.39	2.264	7.796	24.318	βCHN (58), νCCC(32)
30			1313	2.53	2.57	29.46	8.926	βCCC(62), γCHNO (35)
31	1347vs	1345 vs	1356	6.692	7.257	30.555	32.317	νNC(57), νCC(37)
32	1365w		1396	1.689	1.942	12.367	36.441	νCC (71)
33	1440w	1441 vs	1440	1.64	2	3.08	26.15	νCC(68), βCCH (29)
34	1478s	1476 s	1490	2.204	2.886	3.995	11.899	νCC(65), βCCN (34)
35			1510	2.597	3.491	3.183	61.396	νCC(59), νNC (30)
36	1561w	1556 s	1593	5.69	8.5	0.64	62.717	νCC(67), βCCH (26)
37		1612 s	1640	5.676	8.998	6.151	47.329	νCC(55), βCCH (32)
38	1651vs	1657 s	1650	6.128	9.831	13.776	133.428	νCN(68), νCCC(27)
39	1879w		1842	8.41	15.05	516.7	16.977	νOC(74)

(*Contd.*)

Table 5 — Comparison of the experimental (FT−IR and FT−Raman) wavenumbers (cm^{-1}) and calculated wavenumbers (cm^{-1}) of phthalazine-1(2H)-one calculated by B3LYP method. (*Contd*.)

Mode numbers	Experimental		Calculated	Reduced mass (μ)	Force constant (*f*)	IR Intensity (I_{IR})	Raman activity	PED (%) ≥ 10 %
	FTIR	FT-Raman	Frequency					
40	2943s		3010	1.086	6.424	0.556	69.77	ν_{ss} CH(97)
41	3029s	3064 vs	3035	1.091	6.478	3.088	38.856	ν_{ss} CH(92)
42	3103s		3115	1.09	6.49	12.62	90.9543	ν_{as} CH(89)
43	3161vs		3170	1.094	6.562	9.84	89.235	ν_{as} CH(97)
44	3286vw		3295	1.095	6.62	4.892	62.719	ν_{as} CH(92)
45	3466ms		3488	1.07	8.24	81.4	96.458	ν NH (100)

Note: ν: stretching; β: in-plane bending; γ: out-plane bending; ν_{ss}: symmetrical stretching; ν_{as}: asymmetrical stretching; PED: Potential Energy Distribution; s: strong; vs: very strong; w: weak; vw: very weak

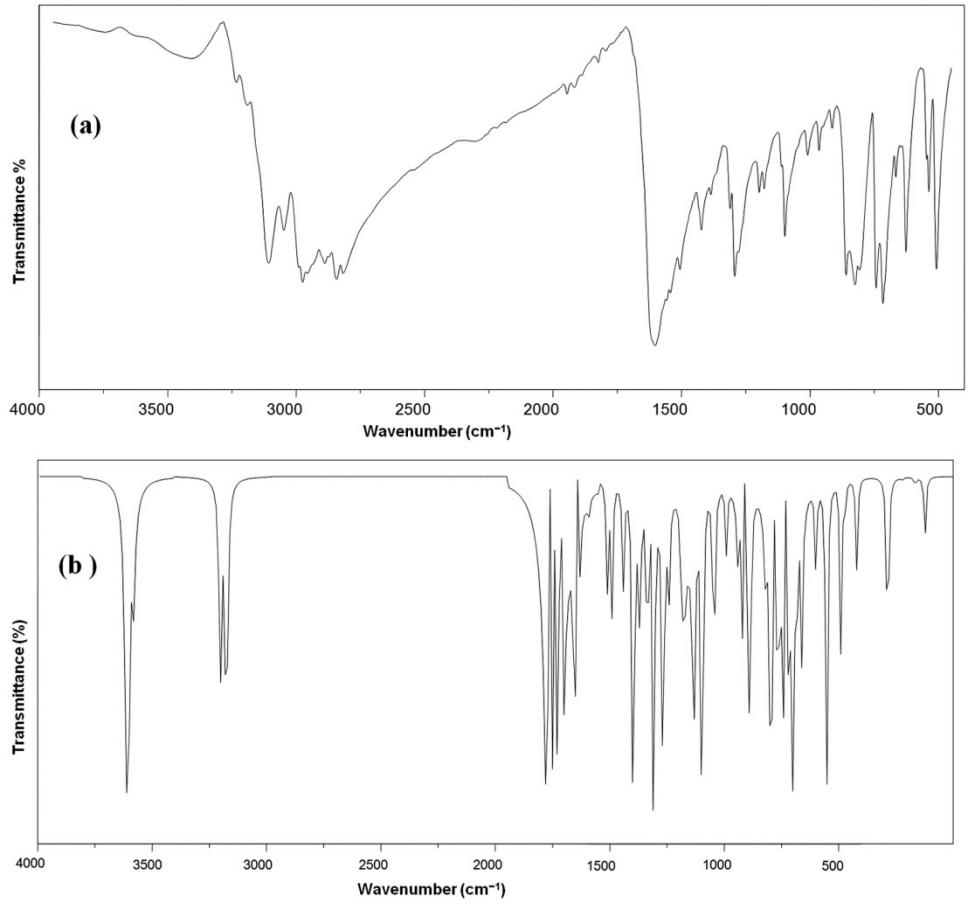

Fig. 6 — (a) Observed and (b) calculated FT-IR spectrum of phthalazine-1(2H)-one.

wave number values higher in comparison to the experimental wave number data. Reduction in the computed harmonic vibrational wave numbers, though basis set sensitive are only marginal as in the DFT values using 6-311++G(d,p). For visual comparison, the observed and simulated FT-IR and FT-Raman spectra of the molecule are presented in Figs 6 (a,b) and 7(a,b), which help to understand the observed spectral features.

5.1 C-H vibrations

In the present study, the five adjacent hydrogen atoms left around the title molecule give rise to five C−H stretching modes (*v44 - v40*), five C−H in-plane bending*(v22, v23, v25- v27)* and five C−H out-of-plane bending (*v13 – v9*) modes. The heteroaromatic organic molecule shows the presence of the C−H stretching vibrations in the 3000 – 3100 cm^{-1} range which is the characteristic region for the identification

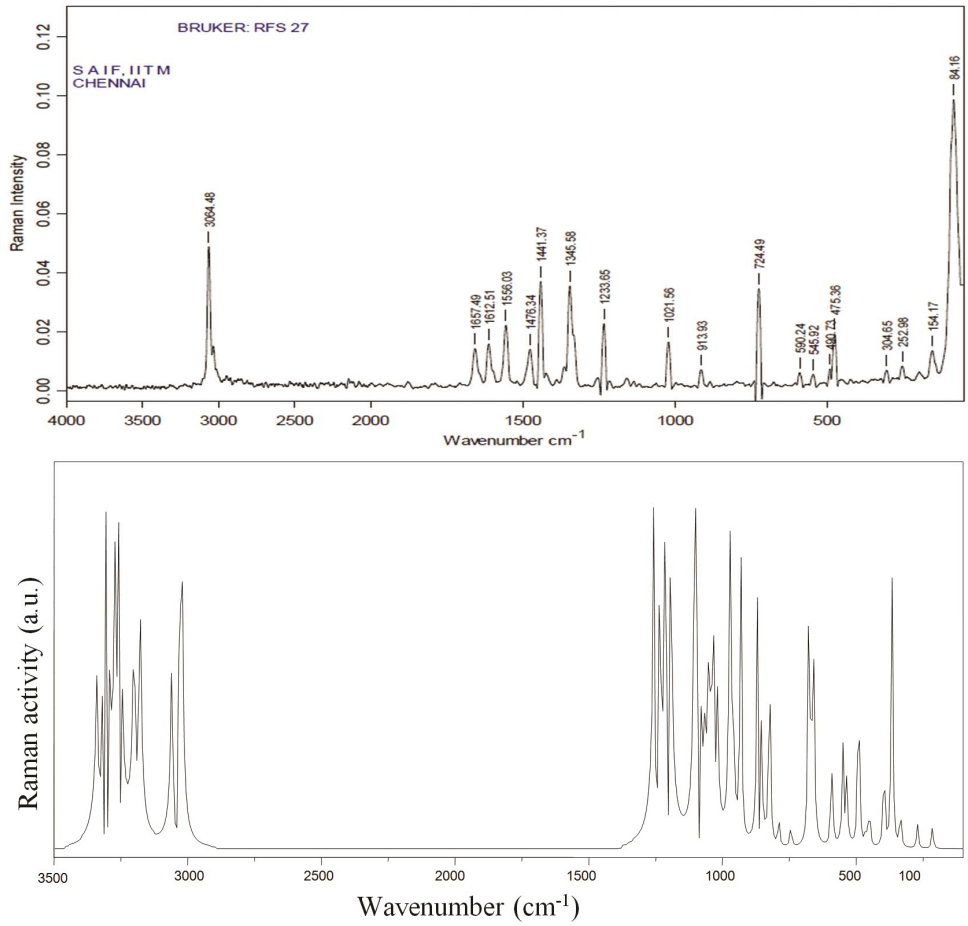

Fig. 7 — (a) Observed and (b) calculated FT-Raman spectrum of phthalazine-1(2H)-one.

of C−H stretching vibrations[28]. Accordingly, the C−H stretching modes of title molecule are assigned to 3286, 3161, 3103, 3029, and 2943 cm^{-1} in FT-IR and very strong band observed at 3064 cm^{-1} in FT-Raman spectrum. These modes are calculated from 3295 to 3010 cm^{-1} for the compound. They are pure modes since their PED contributions are almost 100%. In hetero-aromatic compound, the C-H in-plane and out-plane bending vibrations appear in the range 1000 – 1300 cm^{-1} and 750 – 1000 cm^{-1} respectively[29, 30]. Hence the C−H in-plane bending modes are assigned to 1152, 1064, 1019 cm^{-1} in FT-IR, these peaks are appeared from very strong to medium intense and 1021 cm^{-1} in FT-Raman. The calculated values of this mode are 1152, 1141, 1096, 1044, 1017 cm^{-1} which show better agreement with FT-IR experimental values. The C−H out-of-plane bending vibrations are attributed to 681, 600, 592, 562 cm^{-1} in FT-IR, FT-Raman band of above said vibration observed weak intense at 590, and 540 cm^{-1}. In the present study, the theoretical values of C−H out-of-plane bending modes show good agreement with the experimental values as well as with that of similar kind of molecule[31]. The PED contribution to these modes indicates that, C−H out-of-plane bending modes are mixed mode and these were presented in Table 5.

5.2 CCC vibrations

In case of phthalazine-1(2H)-one ring possesses six ring carbon-carbon stretching vibrations in the region 1460 – 1660 cm^{-1} and 1070 − 1150 cm^{-1}. As revealed by PED, the ring C−C stretching modes are observed at 1561, 1478, 1440, 1365 cm^{-1} in FT-IR and 1612, 1556, 1476, 1441 cm^{-1} in FT-Raman. The in-plane and out-of-plane bending vibrations are generally observed below 1000 cm^{-1} and these modes are not pure but contain a significant contribution from other modes due to substituent-sensitive[31]. In the title molecule, ring in-plane bending mode are observed at 879, 862, 797 cm^{-1} in FT-IR and out-plane bending mode observed at 475, 304 cm^{-1} in FT-Raman. The calculated bands at 470, 468, 420, 285, 121 cm^{-1} are assigned to out-of-plane bending vibrations. The

peak for these modes is not observed in FT-IR spectrum since these modes are possible to appear only in far IR spectrum. The theoretical wave numbers corresponding to ring vibrations are found to have a good correlation with the experimental observations.

5.3 C−N, N−N, and C=O vibrations

The C−N Stretching vibration is difficult to identifying in other group vibrations. The C−N stretching absorption for title compound is identified in the region 1382 – 1266 cm^{-1}. In the present work, the C−N stretching vibrations are observed at 1347 and 1345 cm^{-1} in FT-IR and FT-Raman, respectively. All the bands lie in the expected range when compared to the literature[32, 33]. Consequently, the C−N in-plane and out-of-plane vibrations assigned at 771 cm^{-1} in IR. These assignments are validated by the literature[32–35]. The identification of C−N vibration is a difficult one; it falls in a complicated region of the vibrational spectrum. However, with the help of force field calculations, the C−N vibrations were well identified and assigned in this study.

The experimentally observed band at 1093 cm^{-1} is assigned as N−N stretching vibration for Phthalazine derivatives[36]. In our present case, N−N stretching mode observed medium intensity at 1064 cm^{-1} in FT-IR. The same modes calculated theoretically at 1096 cm^{-1} were show good agreement nearly with experimental value.

Generally C=O group vibrations are observed with very strong intensity in the region[37] 1800 – 1700 cm^{-1}. In our title molecule shows very strong intense IR band at 1879 cm^{-1} assigned to C=O stretching vibration, theoretically calculated band at 1842 cm^{-1} agree with the expected value. The C=O in-plane and out-of-plane bending vibrations are observed at 968 cm^{-1} in FT-IR due to the spectral limit we did not get out-of-plane mode in the IR. The out-of-plane mode observed at 154 cm^{-1} in Raman. The calculated wave number is 164 cm^{-1}.

6 First Hyperpolarizability Calculation

The electric dipole moments (μ) and the first hyperpolarizability (β) tensor components are calculated by DFT/B3LYP/6-311++G(d,p) basis function of the compound so that the relativistic effect of heavy atoms on β were taken into account. All μ and β calculations were performed using GAUSSIAN 03*W*. Those values of Gaussian output are in atomic units (a.u.) so they have been converted into electrostatic units (esu) (α; 1 a.u. = 0.1482×10^{-24} esu, β; 1 a.u. = 8.6393×10^{-33} esu). It is well known that the higher values of dipole moment, molecular polarizability, and hyperpolarizability are important for more active NLO properties. The calculated dipole moment is 3.812 Debye. The highest value of dipole moment is observed for component μ_y. In this direction, this value is − 2.2488 D. The calculated polarizability α_{ij} have non-zero values and was dominated by the diagonal components. Total polarizability (α_{tot}) calculated as 14.635×10^{-24} esu. The first hyperpolarizability value β_{tot} is equal to 0.213×10^{-30} esu. These values are presented in Table 6. The hyperpolarizability β dominated by the components of $\beta_{xzz.}$. Domination of particular component indicates on a substantial delocalization of charges in this direction of title compound. The first hyperpolarizability value (β) responsible for π–electron cloud movement from donor to acceptor which makes the molecule highly polarized and the intramolecular charge transfer possible.

7 Thermodynamic Properties

The thermodynamic functions viz, heat capacity at constant pressure (C_p), Gibb's free energies (G_m), and entropies (S) for the title compound were evaluated from the theoretical harmonic frequencies obtained from B3LYP/6-311++G(d,p) method in the temperature

Table 6 — The electric dipole moment μ (D) the average polarizability α_{tot} ($\times 10^{-24}$ esu) and the first hyperpolarizability β_{tot} ($\times 10^{-31}$ esu) of phthalazine-1(2H)-one.

Parameter	Value	Parameter	Value
μ_x	-3.0789	βxxx	0.3547
μ_y	-2.2488	βxxy	2.686
μ_z	0	βxyy	-29.3649
μ_{Total}	3.812	βyyy	-17.0632
α_{xx}	−56.755	βxxz	0.0004
α_{yy}	−66.398	βxyz	0
α_{zz}	−65.933	βyyz	-0.0001
‹α›	− 63.0287	βxzz	8.9251
α_{tot} (esu)	14.635×10^{-24}	βyzz	2.7466
		βzzz	0.0001
		β_{tot} (esu)	0.213×10^{-30}

Table 7 — The calculated thermodynamic parameters of phthalazine-1(2H)-one by various temperature.

Temperature (K)	Specific heat capacity (C_p)	Gibb's free energy (G_m)	Entropy (S)
200	7.218797	− 3.7037	10.922
300	17.436	−9.7977	27.234
400	32.716	−19.5231	52.2398
500	52.9378	−33.1933	86.131
600	77.745	−50.9632	120.708
700	106.71	−72.8744	179.585

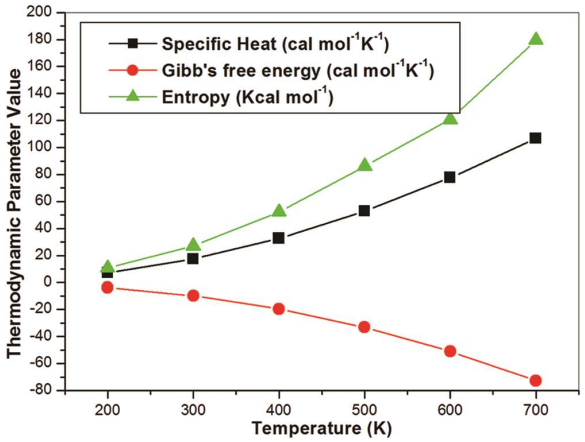

Fig. 8 — Calculated thermodynamical parameter of phthalazine-1(2H)-one.

range 200−700 K and listed in Table 7. From Table 7, it can be observed that these thermodynamic parameters (specific heat (C_p), and entropy (S)) increase with rise of temperature due to the fact that the molecular vibrational intensities increase with temperature[40]. The temperature dependence correlation graphs are shown in Fig.8.

8 Conclusions

In this study, we computed vibrational spectra of phthalazine-1(2H)-one using B3LYP/6-311++G(d,p) method. Any discrepancy noted between the observed and the calculated frequencies may be due to the fact that the calculations have been actually done on a single molecule in the gaseous state contrary to the experimental values recorded in the solid state. Molecular geometry parameters calculated by DFT agree with the experimental values of same molecule and also similar molecule. Information about the size, shape, charge density distribution and site of chemical reactivity of the molecule has been obtained by mapping electron density isosurface with MEP. The lowering of the HOMO - LUMO energy gap value has substantial influence on the intramolecular charge transfer (ICT) and bioactivity of the molecule. FT-IR and Raman spectra were recorded and the vibrational bands were assigned on the basis of the PED calculation. We have concentrated in the structural activity, the description of the molecular docking and MEP surfaces shows same active region in the molecule. Finally, the dipole moment and first hyperpolarizability values may confirm the presence of ICT within the molecule. The charge delocalization and stabilization energies between the lone pair and antibonding orbital's confirm the ICT within the molecule. The dielectric relaxation studies show the existence of molecular interactions between phthalazine-1(2H)-one and alcohol mixture. The increase in concentration of the solute increases the relaxation time which directly depends upon the shape and size of the rotating molecular entities of the solution. The correlation between the statistical thermodynamics and temperature are also obtained. It is seen that the heat capacity (C_p), and entropy (S) increase with the increasing of temperature owing to the intensities of the molecular vibrations increase with increasing temperature.

References

1 Demirayak S, Karaburun A & Beis R, *Eur J Med Chem,* 39 (2004) 1089.
2 Chorghade M S, *In drug discovery and development*, (John Wiley & Sons: Hoboken, New Jersey), 2007.
3 Grasso S, De Sarro G, De Sarro A, Micale N, Zappala M, Puia G, Baraldi M & De Micheli C, *J Med Chem*, 43 (2000) 2851.
4 Nomoto Y, Obase H, Takai H, Teranishi M, Nakamura J & Kubo K, *Chem Pharm Bull,* 38 (1990) 2179.
5 Cardia M C, Distinto E, Maccioni E & Delogu A, *J Heterocycl Chem,* 40 (2003) 1011.
6 Cockcroft X, Dillon K J, Dixon L, Drzewiecki J, Eversley P, Gomes S, Hoare J, Kirrigan F, Natthews I, Menear K A, Martin N M B, Newton R, Paul J, Smith G C M, Vile J & Whittler A, *J Bioorg Med Chem Lett*, 16 (2006) 1040.
7 Cockcroft X, Dillon K J, Dixon L, Drzewiecki J, Kirrigan F, Loh V M, Martin N M B, Menear K A & Smith G, *Bioorg Med Chem Lett,*15 (2005) 2235.
8 Kim J S, Lee H, Suh M, Choo H P, Lee S K, Park H J, Kim C, Park S W & Lee C, *Bioorg Med Chem Lett,* 12 (2004) 3683.
9 Haikal A, El-Ashery E & Banoub J, *Carbohydr Res*, 338 (2003) 2291.
10 Watanabe N, Kabasawa Y, Takase Y, Matsukura M, Miyazaki K, Ishihara H, Kodama K & Adashi H, *J Med Chem,* 41 (1998) 3367.
11 Johnsen M, Rehse K, Petz H, Stasch J & Bischoff E, *Arch Pharmacol,* 336 (2003) 591.
12 Madhavan G R, Chakrabarti R, Kumar S K, Misra P, Mamidi R N, Balraju V, Ksiram K, Babu R K, Suresh J, Lohray B B, Lohray V B, Iqbal J & Rajagopalan R, *Eur J Med Chem*, 36 (2001) 627.
13 Cashman J R, Voelker T, Johnson R, & Janowsky A, *Bioorg Med Chem,* 17 (2009) 337.
14 Frisch M J,Trucks G W & Schlegal H B, *GAUSSIAN 09, Revision A.02, Gaussian, Inc, Pittsburgh, PA*, 2009.
15 Pulay P, Fogarasi G, Pongor G, Boggs J E & Vargha A, *J Am Chem Soc*, 105 (1983) 7037.
16 Sundius T, *J Mol Struct*, 218 (1990) 321.
17 Sundius T, *Vib Spectrosc*, 29 (2002) 89.
18 Sangeetha C C, Madivanane R & Pouchaname V, *Int J Eng Res Gen Sci*, 2(6) (2014) ISSN 2091.
19 Gupta V P, Sharma A, Virdi V & Ram V J, *Spectrochim Acta*, 64A (2006) 57.

20 Powell B J, Baruah T, Bernstein N, Brake K, McKenzie R H, Meredith P & Pederson M R, *J Chem Phys,* 120 (2004) 8608.
21 Karakurt T, Dinçer M, Çetin A & Sekerci M, *Spectrochim Acta*, 77A (2010) 189.
22 Choi C H & Kertesz M, *J Phys Chem*, 101A (1997) 3823.
23 Smith D W, *J Chem Soc Faraday Trans*, 94 (1998) 201.
24 Parr R G, Von Szentpaly L & Liu S, *J Am Chem Soc*, 121 (1999) 1922.
25 Pawar V P & Mehrotra S C, *J Mol Liq*, 95 (2002) 63.
26 Savage P E, *Chem Rev*, 99 (1999) 603.
27 Mulliken R S, *J Chem Phys*, 23 (1955) 1833.
28 Silverstein M, Clayton Basseler G & Morill C, *Spectromet Ident Org Comp*, Wiley, New York, 1981.
29 Socrates G, *Infrared characteristic group of frequencies*, (Wiley: New York), 1980.
30 Varasanyi G, *Assignments of vibrational spectra of seven hundred benzene derivatives*, (Wiley: New York), 1974.
31 Roeges N P G, *A guide to the complete interpretation of infrared spectra of organic structures*, (Wiley: New York), 1994.
32 Krishnakumar V & Balachandran V, *Spectrochim Acta*, 61A (2005) 1001.
33 Medhi K C, Barman R & Sharma M K, *Indian J Phys*, 68B (1994) 189.
34 Smith B, *Infrared spectral interpretation*: *A systematic approach*, (CRC Press: Washington, DC), 1999.
35 Sathyanarayana D N, *Vibrational spectroscopy – Theory and applications*, second ed, (New Age International (P) Limited Publishers: New Delhi), 2004.
36 Panicker C Y, Ambujakshan K R, Varghese H T, Mathew S, Ganguli S, Nanda A K & Van Alsenoy C, *J Raman Spectrosc*, 40 (2009) 527.
37 Peesole R L, Shields L D, Cairus I C & Willam M C, *Modern method of chemical analysis*, (Wiley: New York), 1976.
38 Sun Y X, Hao Q L, Wei W X, Yu Z X, Lu L D, Wang X & Wang Y S, *J Mol Struct*, 904 (2009) 74.
39 Reis H, Papadopoulos M G & Munn R W, *J Chem Phys*, 109 (1998) 6828.
40 Ott J B, *J boerio-goates, calculations from statistical thermodynamics*, (Academic Press), 2000.